# Additional records and stratigraphic distribution of the middle Eocene carettochelyid turtle *Anosteira* pulchra from the Uinta Formation of Utah, North America (#49966)

First submission

#### Guidance from your Editor

Please submit by 25 Jun 2020 for the benefit of the authors (and your \$200 publishing discount).



#### **Structure and Criteria**

Please read the 'Structure and Criteria' page for general guidance.



#### **Custom checks**

Make sure you include the custom checks shown below, in your review.



#### Raw data check

Review the raw data.



#### Image check

Check that figures and images have not been inappropriately manipulated.

Privacy reminder: If uploading an annotated PDF, remove identifiable information to remain anonymous.

#### **Files**

Download and review all files from the <u>materials page</u>.

7 Figure file(s) 2 Table file(s)

Custom checks

#### Field study

Have you checked the authors field study permits?

Are the field study permits appropriate?

## Structure and Criteria



#### Structure your review

The review form is divided into 5 sections. Please consider these when composing your review:

- 1. BASIC REPORTING
- 2. EXPERIMENTAL DESIGN
- 3. VALIDITY OF THE FINDINGS
- 4. General comments
- 5. Confidential notes to the editor
- Prou can also annotate this PDF and upload it as part of your review

When ready <u>submit online</u>.

#### **Editorial Criteria**

Use these criteria points to structure your review. The full detailed editorial criteria is on your guidance page.

#### **BASIC REPORTING**

- Clear, unambiguous, professional English language used throughout.
- Intro & background to show context.
  Literature well referenced & relevant.
- Structure conforms to <u>PeerJ standards</u>, discipline norm, or improved for clarity.
- Figures are relevant, high quality, well labelled & described.
- Raw data supplied (see <u>PeerJ policy</u>).

#### EXPERIMENTAL DESIGN

- Original primary research within Scope of the journal.
- Research question well defined, relevant & meaningful. It is stated how the research fills an identified knowledge gap.
- Rigorous investigation performed to a high technical & ethical standard.
- Methods described with sufficient detail & information to replicate.

#### **VALIDITY OF THE FINDINGS**

- Impact and novelty not assessed.
  Negative/inconclusive results accepted.
  Meaningful replication encouraged where rationale & benefit to literature is clearly stated.
- All underlying data have been provided; they are robust, statistically sound, & controlled.
- Speculation is welcome, but should be identified as such.
- Conclusions are well stated, linked to original research question & limited to supporting results.

## Standout reviewing tips



The best reviewers use these techniques

Τ	p

## Support criticisms with evidence from the text or from other sources

### Give specific suggestions on how to improve the manuscript

### Comment on language and grammar issues

### Organize by importance of the issues, and number your points

## Please provide constructive criticism, and avoid personal opinions

Comment on strengths (as well as weaknesses) of the manuscript

#### **Example**

Smith et al (J of Methodology, 2005, V3, pp 123) have shown that the analysis you use in Lines 241-250 is not the most appropriate for this situation. Please explain why you used this method.

Your introduction needs more detail. I suggest that you improve the description at lines 57-86 to provide more justification for your study (specifically, you should expand upon the knowledge gap being filled).

The English language should be improved to ensure that an international audience can clearly understand your text. Some examples where the language could be improved include lines 23, 77, 121, 128 - the current phrasing makes comprehension difficult.

- 1. Your most important issue
- 2. The next most important item
- 3. ...
- 4. The least important points

I thank you for providing the raw data, however your supplemental files need more descriptive metadata identifiers to be useful to future readers. Although your results are compelling, the data analysis should be improved in the following ways: AA, BB, CC

I commend the authors for their extensive data set, compiled over many years of detailed fieldwork. In addition, the manuscript is clearly written in professional, unambiguous language. If there is a weakness, it is in the statistical analysis (as I have noted above) which should be improved upon before Acceptance.



## Additional records and stratigraphic distribution of the middle Eocene carettochelyid turtle *Anosteira pulchra* from the Uinta Formation of Utah, North America

Brent Adrian Corresp., 1, Patricia A. Holroyd 2, J. Howard Hutchison 2, K.E. Beth Townsend 1

Corresponding Author: Brent Adrian Email address: badria@midwestern.edu

**Background.** Anosteira pulchra is one of two species of the obligately-aquatic freshwater clade Carettochelyidae (pig-nosed turtles) from the Eocene of North America. A. pulchra is typically rare in collections, and their distribution is poorly documented. The Uinta Formation [Fm.] contains diverse assemblages of turtles from the Uintan North American Land Mammal Age (NALMA). Whereas turtles are abundantly preserved in the Uinta Fm., A. pulchra has been reported only from a few specimens in the Uinta C Member.

**Methods.** We describe new records of *Anosteira pulchra* from the Uinta Basin and analyze the distribution of 95 specimens from multiple repositories in the previously published stratigraphic framework of the middle and upper Uinta Fm.

**Results.** Here we report the first records of the species from the Uinta B interval, document it from multiple levels within the stratigraphic section and examine its uncommon appearance in only approximately 5% of localities where turtles have been systematically collected. This study details and extends the range of *A. pulchra* in the Uinta Fm. and demonstrates the presence of the taxon in significantly lower stratigraphic layers. These newly described fossils include previously unknown elements and associated trace fossils, with new anatomical information presented.

<sup>1</sup> Department of Anatomy, Midwestern University, Glendale, Arizona, United States

<sup>&</sup>lt;sup>2</sup> Museum of Paleontology, University of California, Berkeley, Berkeley, California, United States



- Additional records and stratigraphic distribution of
- the middle Eocene carettochelyid turtle *Anosteira*
- 3 pulchra from the Uinta Formation of Utah, North
- 4 America

5	
6	Brent Adrian <sup>1</sup> , Patricia A. Holroyd <sup>2</sup> , J. Howard Hutchison <sup>2</sup> , K.E. Beth Townsend <sup>1</sup>
7	
8	<sup>1</sup> Department of Anatomy, Midwestern University, Glendale, Arizona, USA
9	<sup>2</sup> Museum of Paleontology, University of California, Berkeley, California, USA
10	
11	Corresponding Author:
12	Brent Adrian <sup>1</sup>
13	19555 North 59th Avenue, Glendale, Arizona, 85308, USA
14	Email address: badria@midwestern.edu
15	
16	
17	
18	
19	
20	
21	
22	



#### **Abstract**

24 **Background.** Anosteira pulchra is one of two species of the obligately-aquatic freshwater clade 25 Carettochelyidae (pig-nosed turtles) from the Eocene of North America. A. pulchra is typically rare in collections, and their distribution is poorly documented. The Uinta Formation [Fm.] 26 27 contains diverse assemblages of turtles from the Uintan North American Land Mammal Age 28 (NALMA). Whereas turtles are abundantly preserved in the Uinta Fm., A. pulchra has been 29 reported only from a few specimens in the Uinta C Member. Methods. We describe new records of *Anosteira pulchra* from the Uinta Basin and analyze the 30 distribution of 95 specimens from multiple repositories in the previously published stratigraphic 31 32 framework of the middle and upper Uinta Fm. 33 **Results.** Here we report the first records of the species from the Uinta B interval, document it 34 from multiple levels within the stratigraphic section and examine its uncommon appearance in only approximately 5% of localities where turtles have been systematically collected. This study 35 36 details and extends the range of A. pulchra in the Uinta Fm. and demonstrates the presence of the taxon in significantly lower stratigraphic layers. These newly described fossils include 37 38 previously unknown elements and associated trace fossils, with new anatomical information presented. 39

40

41

#### Introduction

The Uinta Formation [Fm.] in the Uinta Basin of northeastern Utah (Fig. 1) contains a rich and 42 43 diverse assemblage of turtles from the late middle Eocene Uintan NALMA (Lutetian). Anosteira is a genus of small to medium-sized highly aquatic freshwater turtles belonging to 44 Carettochelyidae (Gill, 1889) that apparently emigrated from Asia to North America during the 45



47

48

49

50

51

52

53

54

55

56

57

58

59

60

61

62

early Bridgerian NALMA (Hutchison, 1998). Two North American species of the genus have been described to date. The older of the two, *Anosteira ornata*, is known from several Bridgerian sites in southwest Wyoming (see *Jovce*, 2014 for a recent summary). Gilmore (1916) provisionally reported A. ornata in Uinta C based on CM 2954, collected on the White River near Ouray, Utah. Clark (1932) named Pseudanosteira pulchra based on CM 11808 from the Uinta C horizon at Leota Ranch, northwest of Ouray, Utah, but did not mention CM 2954. Broin (1977) recombined P. pulchra as A. pulchra, noting the differentiation of Pseudanosteira from Anosteira on the shape of the anterior neurals, but reduction of the vertebral scales was not supportable in the absence of data on individual and specific variability. This synonymy was followed by Joyce (2014), Joyce, Volpato & Rollot (2018), and is followed here. Joyce (2014) noted the potential range extension represented by CM 2954 but did not elect to make a species assessment. As the literature currently stands, only two carettochelyid specimens have been noted or described from the Uinta Basin. Both occur in the upper part of the Uinta Fm., in beds historically referred to Horizon C or Uinta C, and may represent two different species. However, targeted collecting in recent years of Uintan herpetofauna in a measured stratigraphic framework has yielded 95 carettochelyid specimens. The aim of this study is to describe the stratigraphic and geographic distribution of A. pulchra in the Uinta Fm. and provide new anatomical information on its morphology.

64

65

66

67

68

63

#### **Geological Setting**

The Uinta Basin in northeastern Utah (*Fig. 1*) is approximately 135 miles wide along its east-west axis and 100 miles across from north to south, encompassing an area of 10, 943 km<sup>2</sup> (*Ryder, Fouch & Elison, 1976; Prothero, 1996; Murphey et al., 2011*). Its boundaries include the



69 Uinta Mountains to the north, the Book Cliffs/Tavaputs Plateau to the south, the Douglas Creek Arch and Roan Plateau to the east, and the Wasatch Range to the west (Murphey et al., 2011) 70 (Fig. 1). Over 4.500 m of Eocene sediments accumulated during the Laramide orogenesis, filling 71 72 the Uinta, Green River, and Piceance Creek basins (Prothero, 1996; Murphey et al., 2011). 73 These sediments record part of a vast system of middle Eocene lakes that covered a large portion 74 of northeastern Utah, southwestern Wyoming, and western Colorado (Ryder, Fouch & Elison, 75 1976; Prothero, 1996; Murphey et al., 2011; Chamberlain et al., 2012). 76 During the Bridgerian NALMA (47-49 Ma), the Green River lake system began to recede, 77 replacing lacustrine shales with fluvial-deltaic mudstones and sandstones which now comprise a rich matrix for terrestrial fossil vertebrates (Murphey et al., 2011). In the Uinta Basin, the fluvial 78 79 Uinta Fm. gradually replaced the Green River lake system, beginning at the east end of the basin 80 (Fig. 1). As a result, the lower fluvial sandstones of the eastern Uinta Fm. are laterally equivalent 81 to lacustrine evaporates, sandstones, and limestones in the western Uinta Basin, and the two units 82 share complex interfingering (Dane, 1954, 1955; Ray, Kent & Dane, 1956; Cashion, 1967; Ryder, Fouch & Elison, 1976). The primary focus of this study is to describe the stratigraphic 83 distribution of *Anosteira pulchra* in the eastern Uinta Fm., and we record some additional 84 85 western occurrences (Fig. 1). 86 The Uinta Fm. is the highly fossiliferous type formation of the Uintan NALMA (Wood et 87 al., 1941; Prothero, 1996) (Figs. 1, 2A). The study area lies between latitudes 40°00' and 40°30' 88 north and longitudes 109°00' and 109°45' west (Townsend, Friscia & Rasmussen, 2006) (Fig. 1). Most of the localities discussed here are tied to a stratigraphic section by Townsend, Friscia 89 90 & Rasmussen (2006) that extends 366 m through the older Uinta B (0-137 m) into the younger 91 Uinta C (140-366 m), resulting in the first conformable contact between the Uinta and Duchesne



107	Materials & Methods
106	
105	Prothero, 1996).
104	150 meters of the formation does not bear fossils (Osborn, 1895; Riggs, 1912; Osborn, 1929;
103	for the lower levels of Uinta B, and many workers have concluded that the lowest approximately
102	baenids was unable to confirm its presence (Smith et al., 2017). Uinta A has often been mistaken
101	(Leidy, 1871), which was reestablished by Joyce & Lyson (2015), but a recent survey of Uintan
100	contain all other reported taxa (Gilmore, 1916). B.inflata has been grouped with "Baena" affinis
99	Only one turtle (Baena inflata) is reported from Uinta A, while Uinta B and C combined
98	Townsend & Holroyd, 2020) (Fig. 2).
97	with them (Gunnell et al., 2009; Townsend et al., 2010; Smith et al., 2017, 2020; Stidham,
96	area of the stratotype localities for biochrons Ui2 and Ui3 or can be stratigraphically correlated
95	Uinta, Bridger, and Washakie Formations. Material in the current study occurs in the immediate
94	biochronological zones (Ui1a, Ui1b, Ui2, Ui3) on the basis of mammalian biostratigraphy of the
93	Rasmussen, 2006) (Fig. 2A). Gunnell et al. (2009) divided the Uintan NALMA into four
92	River Formations at 366 m (Osborn, 1895, 1929; Prothero, 1996; Townsend, Friscia &

108 We used measured stratigraphic sections from Townsend, Friscia & Rasmussen (2006), which were recorded during the summers of 1997, 1998, 2000, and 2014. Fossil collection and 109 stratigraphic work was conducted in a restricted area of the eastern Uinta Basin, on public land 110 administered by the Bureau of Land Management. This study includes specimens from the 111 Carnegie Museum of Natural History and the Yale Peabody Museum of Natural History and 112 113 examines previously unpublished specimens from Brigham Young University Museum of Paleontology, the Natural History Museum of Utah, and the Utah Field House of Natural History 114



115 State Park Museum. Collections from the latter three museums were integrated into the measured stratigraphy of Townsend, Friscia & Rasmussen (2006) from locality data on file at each 116 repository. Additional records have been included from the University of California Museum of 117 118 Paleontology from elsewhere in the basin, but these cannot be included in the detailed 119 stratigraphic framework. Measurements of fossil specimens were taken using Mitutoyo Absolute 120 Digimatic digital calipers, and from high quality digital images using ImageJ software (Rasband, 1997-2016). Magnified photos were produced using an Olympus SZX7 stereo microscope. 121 Unless otherwise specified, all measurements are in millimeters (mm), recorded to the nearest 122 123 0.01 mm and rounded to the nearest 0.1 mm. Nomenclature for vertebral scales conforms to that proposed by Danilov et al. (2017). 124

#### **Abbreviations**

126 BYU, Brigham Young University Museum of Paleontology, Provo, Utah, USA; CM, Carnegie Museum of Natural History, Pittsburgh, Pennsylvania, USA; MWU, Midwestern 127 128 University, Glendale, Arizona, USA; UCMP, University of California Museum of Paleontology, 129 Berkeley, California, USA; UFH, Utah Field House of Natural History State Park Museum, 130 Vernal, Utah, USA; UMNH.VP, Vertebrate Paleontology Collection, Natural History Museum 131 of Utah, Salt Lake City, Utah, USA; WU, Washington University, St. Louis, Missouri, USA; YPM VPPU, Princeton University collection in the Division of Paleontology, Yale Peabody 132 Museum of Natural History, New Haven, Connecticut, USA. ne= neural, nu= nuchal, py= pygal, 133 134 sp= suprapygal.

135

136

125

#### **Systematic Paleontology**

137 TESTUDINES Batsch, 1788

#### **PeerJ**

138	CRYPTODIRA Cope, 1868
139	TRIONYCHIA Hummel, 1929
140	CARETTOCHELYIDAE Gill, 1889
141	ANOSTEIRA Leidy, 1871
142	Anosteira pulchra (Clark, 1932)
143	Figures 3-6; Tables 1-2
144	Synonymy. Pseudanosteira pulchra (Clark, 1932)
145	Holotype. CM 11808, a complete carapace, nearly complete hyoplastra, hypoplastra, and anterior
146	extremities of posterior plastral lobe.
147	Newly Referred Specimens. See <i>Table 1</i> .
148	Type Locality and Horizon. Quarry L, Leota Ranch, near village of Ouray, Uinta County, Utah,
149	USA (Clark, 1932, figure 7). Upper Horizon C (Clark, 1932:161), Uinta Formation, Lutetian,
150	middle Eocene.
151	Description
152	Due to the large sample size in this study, the specimens described below were selected as
153	representative elements of A. pulchra found within the measured stratigraphic section of
154	Townsend, Friscia & Rasmussen (2006).
155	Carapace (Fig. 3)
156	UMNH.VP.27632 is an anterior carapace margin that includes the nuchal and left first
157	peripheral (Fig. 3A-B). There is a midline protuberance approximately 7 mm wide and 5 mm
158	long that is raised 1.5 mm above the dorsal surface of the carapace, occupying most of the
159	midline space between the anterior free margin and the intervertebral sulcus between the fused
160	cervical/vertebral 1 and vertebral 2 scales (Fig. 3A). The protuberance forms the anterior limit of



162

163

164

165

166

167

168

169

170

171

172

173

174

175

176

177

178

179

180

181

182

183

the dorsal keel, and a rounded dorsal projection is the most robust point along the thickened margin of the nuchal embayment (Fig. 3A). The anterior extremities of the sulci forming the slightly sigmoidal lateral sides of vertebral scale 2 project posteriorly from the aforementioned intervertebral sulcus (Fig. 3A). The sulci of this element are generally thin (< 0.5 mm) and finely incised (Fig. 3A). Dorsal surface sculpture consists of a network of grooves that are roughly parallel to the free margin of the carapace (Fig. 3A). Grooves are shorter, more clustered, and have more pronounced relief where the periphery changes direction, as at peripheral 1 (Fig. 3A). The dorsal surface is quite smooth near the midline of the nuchal, where a slight ridge indicates the beginning of the median keel (Fig. 3A). The ventral surface of UMNH.VP.27632 is smooth except for finely toothed sutures between the specimen and adjacent bones (Fig. 3A-B). A pair of gracile projections extend from the internal surface of the carapace to articulate with cervical vertebra 8 (Fig. 3B). Each projection is approximately 2.4 mm wide, 1 mm long, and 1.7 mm tall, crescent-shaped, and concave posteriorly (Fig. 3B). UMNH.VP.31059 (Fig. 3C) and UMNH.VP.27146 (Fig. 3D-F) are partial anterior neural rows of A. pulchra, with a characteristic anterior spike in the midline carina (keel) arising from neurals 3 and 4 (Fig. 3C-D). The spike falls sharply in the posterior third of neural 4, returning to approximately the same maximum height as the midpoint of neural 4 (Fig. 3C-D). Neural 5 of UMNH.VP.27146 is missing (Fig. 3D-F), though the keel of neural 6 was likely similar in height (Fig. 3D). UMNH.VP.30590 (Fig. 3G-L) consists of associated posterior midline elements (neurals 6 and 7, suprapygal, and pygal), as well as peripheral 8 described below (Fig. 3Y-AA). Neural 6 is generally tectangular dorsally, measuring 7.5 mm long and 4.2 mm wide (Fig. 3G-H). Neural 7 is proportionally shorter, and is 8.1 mm long and 6.2 mm wide (Fig. 3G-H). The dorsal outline



185

186

187

188

189

190

191

192

193

194

195

196

197

198

199

200

201

202

203

204

205

206

of neural 7 is distinctly hexagonal, and its surface area is larger dorsally than ventrally (Fig. 3G-H). Both posterior neurals have a smooth dorsal surface, and the posterior keel of neural 6 is warped slightly laterally (Fig. 3G). The keel of neural 6 is triangular in profile and forms a second spike behind that of neural 4, rising approximately 3 mm above the external surface (Fig. 31). Midline parts of UMNH.VP.30590 are missing between the posteriormost neurals and suprapygal (Fig. 3G-L). The eighth costals are missing, but meet at the midline in situ in complete specimens (see *Hay*, 1908; *Clark*, 1932; *Danilov et al.*, 2017). A tightly beaded pattern covers the dorsal and ventral surfaces of the pygal posterior to the anterior ventral embankment (Fig. 3J-L). The posterior pygal margin is acute, similar to the posterior peripherals, but is thickest at the midline (Fig. 3J-L, AA). The pygal has a midline sulcus along the dorsal surface, as described above (Fig. 3J). A low keel bisects the suprapygal along the dorsal midline, and the ventral surface of the suprapygal is smooth and slightly concave (Fig. 3J-K). The suture between the suprapygal and pygal is finely dentate (Fig. 3K), and the pygal flares posteriorly and dorsally (*Fig. 3J-L*). UMNH.VP.19951 is a right costal 1 that is missing two sections of its posterior edge (Fig. 3M-N). It has a length of 21.9 mm and a width of 41.2 mm. Its posterior suture is concave anteriorly, and its anterior margin convex, where it is sutured for articulation with the nuchal and the first three peripherals (Fig. 3.M-N). The medial and lateral sutures are preserved, indicating articulation with neural 1 and the anterior portion of peripheral 3, respectively (Fig. 3N). The bone is thinnest near its middle, and the head of the first rib is separated from the medial suture and flanked by several small foramina (Fig. 3N). Otherwise, the ventral surface is smooth, and the dorsal surface shows little evidence of texture apart from a few oblong pits and small gouges (*Fig. 3M*).



207 UMNH.VP.31058 is a right peripheral 2 that has the characteristic flattened cylindrical shape of the anteriormost peripherals (Fig. 30-Q). Its lateral edge is straight (Fig. 30-P), and the 208 209 lateral margin is rounded in cross section (Fig. 30). No sulci are present, and a finely pitted 210 texture is present only in dorsal view (Fig. 30). The surface becomes smooth along the lateral 211 edge and ventral view of the bone (Fig. 3P). UMNH.VP.27077 is a left peripheral 3 that is missing its anteromedial corner (Fig. 3R-212 S). Its ventral surface is smooth (Fig. 3S), and its dorsal surface is slightly rugose and damaged 213 by two large, irregular pits near the lateral edge (Fig. 3R). The posterolateral margin projects 214 215 ventrally and there are two prominent sockets that mark articulation with the hypplastron and the 216 beginning of the bridge series of peripherals (Fig. 3S). The anterior half of the lateral margin maintains the flattened cylindrical character of the peripherals anterior to it, but the edge slopes 217 sharply ventrally as it forms the seat of the axillary buttress of the bridge (Fig. S-T). 218 219 UMNH.VP.27077 also includes a left peripheral 6 with robust gomphotic sockets that characterize bridge peripherals (Fig. 3U-X). Anteriorly, peripherals are thin and rod-like (Fig. 220 221 30-0), become thick and triangular in the bridge region (Fig. 3R-X), and are wide and flat 222 posteriorly (Fig. 3Y-AA). Peripheral 8, associated with other elements from UMNH.VP.30590 223 described above (Fig. 3G-L), is an example of the broad, flat, acutely-margined posterior peripherals (Fig. 3Y-AA). It is 19.2 mm long, 18.1 mm wide, and 9.77 mm tall, and only its 224 dorsal surface is sculptured (Fig. 3Y). An intermarginal sulcus crosses the dorsal surface 225 226 transversely at its anterior third (Fig. 3Y), and a longitudinal, rounded embankment tapers posteriorly along the medial side of the ventral surface (Fig. 3Z). 227 To summarize, peripherals articulate to form a slightly flaring, often scalloped ring whose 228 229 most distal parts are thin and delicate (Figs. 3Y-AA, 6B, D). Distinct gomphoses indicate clear



articulations between bridge peripherals 3-7 and adjacent bones of the carapace and plastron (*Fig. 3T, X*), while anterior peripherals 1-2 and posterior peripherals 8-10 only articulate with the carapace (*Fig. 3Q, AA*). The angle formed by the dorsal and ventral faces at the lateralmost edge of the shell is approximately 66.5° in peripheral 6 (*Fig. 3X*), but becomes acute to approximately 28° in the posterior peripherals (*Fig. 3AA*). A distinct median dorsal carina (keel) forms a blunt, posteriorly-oriented spike on neurals 3-4 (*Clark, 1932*) (*Fig. 3C-E*). The carina continues posteriorly and terminates on the antero-dorsal view of the pygal as a distinctly raised midline ridge anterior to the confluence of the marginal scales (*Fig. 3J*). The pygal is robust and trapezoidal (*Fig. 3J-K*). It has a pronounced embankment perpendicular to the midline in anteroventral view, as in all carettochelyids, forming a posterior wall of the body cavity (*Havlik, Joyce & Böhme, 2014; Joyce, 2014*) (*Fig. 3K-L*).

#### Plastron (Fig. 4)

UMNH.VP.19551 is an articulated left hyo- and hypoplastron that displays a classic reduced "cruciform" plastron (*Fig. 4A-B*). It is missing a portion of the anteromedial corner of the hypoplastron, and the anterior and posterior parts of the bridge region (*Fig. 4A-B*). The maximum length of the specimen is 31.9 mm, of which 18.5 mm accounts for the hypoplastron. Its overall maximum width is 40.7 mm, and the hypo-xiphiplastral suture is 9.2 mm wide. The bridge region is flattened and the hypoplastron is longer than the hypoplastron at their narrowest points (*Fig. 4A-B*). The ventral surface is smooth near the midline and rugose at the middle of the specimen, with parallel striations projecting toward the bridge articulation (*Fig. 4A*). The dorsal surface is smooth except for short grooves near the bridge and raised red concretions in the hyo-hypoplastral suture (*Fig. 4B*). The anterior edge of the hypoplastron forms a rounded "M" shape, with larger medial and smaller lateral, anteriorly-projecting projections that form the seat



253	for the epiplastron (Fig. 4A-B). The medial projection is finely pitted along its anterior edge,
254	likely for ligamentous attachment to the epiplastron and entoplastron (Fig. 4A-B). It is notable
255	that the hypo-xiphiplastral suture of UMNH.VP.19551 (Fig. 4A-B) is relatively straight,
256	compared with the sinusoidal sutures of the specimens described below, though this may be
257	attributable to breakage (Fig. 4C-I).
258	UMNH.VP.27452 is a nearly complete left hypoplastron (Fig. 4C-D). The bridge region
259	is fractured at its narrowest, central point (8.8 mm wide) (Fig. 4C-D). The hyo-hypoplastral
260	suture is visible along the bone's anteromedial edge, where the bone is thinnest (2.9 mm) (Fig.
261	4C-D). The sutures of this area are better preserved in the smaller left hypoplastron
262	UMNH.VP.26554 (Fig. 4E-G) and the sutures shared with adjacent bones are intact (Fig. 4E-G)
263	In UMNH.VP.26554, the hyo-hypoplastral suture and the midline form an approximately 73°
264	angle (Fig. 4E, G). The width of the left hypo-xiphiplastral suture is 12.39 mm and the plastron
265	has a maximum thickness of 6.2 mm (Fig. 4E-G). The partial right hypoplastron
266	UMNH.VP.26917 is 24.2 mm long and 14.8 mm wide. Its ventral surface has perhaps the
267	clearest defined texture of all the plastra examined in this study (Fig. 4H). On it, there is a series
268	of four distinct, nearly parallel trace marks on the ventral surface of UNMH.VP.26917,
269	immediately anterior to the hypo-xiphiplastral suture (Figs. 4H, 6). These are interpreted and
270	discussed below.
271	UMNH.VP.20525 is a nearly complete right xiphiplastron that is 32.2 mm long and 11.5
272	mm wide (Fig. 4J-M). The bone is narrow and its lateral edge is nearly parallel to the midline,
273	but its posterior quarter tapers to a point (Fig. 4J-K) indicating the lack of anal notch as in other
274	Anosteira spp. The hypo-xiphiplastral suture is sinusoidal, and the articular surface along the
275	suture is comprised of a complex network of gomphotic scarph pegs and sockets (Fig. 4J-M). It



is generally even in thickness, but is thickest anteriorly along the midline (Fig. 4L). The bone bends dorsally and its posterior point forms a distinct spike with several longitudinal ridges on the dorsal surface (Fig. 4K). Both the dorsal and ventral surfaces are mostly smooth, and several small foramina are present in the anterior half of the dorsal side (Fig. 4K). A narrow groove runs along the posterior end of the lateral side of the bone, which is thinnest near its middle (Fig. 4M). This groove probably marks the limit of the skin contact on the dorsal surface.

#### An associated carapace and plastron (UMNH.VP.31072) (Fig. 6)

One specimen from the current sample has been recovered with an associated carapace and plastron (*Fig.* 6). The carapace consists of a mostly complete neural row, including neurals 2-6 and adjacent costals (*Fig.* 6A, C), along with a peripheral ring that is missing only the left peripheral 3, right peripheral 5, and significant portions of bilateral peripherals 4 and 8 (*Fig.* 6B, D). Neurals 1 and 7 are missing, though most of the suprapygal is preserved including its midline keel (*Fig.* 6A, C). Apart from the medial portions which articulate with the neural series (*Fig.* 6A, C), the costals were fractured into dozens of tiny fragments from the middle of the bones.

The plastron of UMNH.VP.31072 is well preserved, missing only the anterior half of the right xiphiplastron, approximately the posterior third of the left xiphiplastron, and lateral portions of the bilateral hyoplastra (*Fig. 6B, D*). The anterior plastral lobe is represented by one fragment of the epiplastron which articulates with the curved anteromedial margin of the hyoplastron (*Fig. 6B, D*). This posterior portion of the right epiplastron is thickest along a ridge at the middle of the width of the bone, and a narrow groove lies along the medial side of the ridge (*Fig. 6B*). There are fine striations near the midline, anterior to the groove, possibly indicating ligamentous articluation associated with the kinetic hinge at the epi-hyoplastral contact (*Fig. 6B*). The remainder of the plastron is consistent with the specimens described above, and the preserved



right xiphiplastron tapers to a thickened point posteriorly, as in UMNH.VP.20525 (*Fig. 4J-M*). This specimen is the most complete individual of *Anosteira pulchra* in the current study and allows a simple estimation of the turtle's size. Using relative proportions from the type specimen (CM 11808) (*Fig. 7A*), UMNH.VP.31072 is estimated to have a midline carapace length of 15.3 cm, approximately 80% the size of CM 11808.

#### Results

We identified 95 specimens of *Anosteira pulchra* from the Uinta Fm. (*Table 1*) and analyzed their distribution in the stratigraphic framework of *Townsend, Friscia & Rasmussen* (2006) (*Fig. 2*). The results of this analysis substantially increase the sample of Uintan *A. pulchra* and provide new insights into the stratigraphic distribution of the uncommon, obligately aquatic turtle *A. pulchra*. We report most occurrences from Uinta C and extend the stratigraphic range of the species into older Uinta B sediments. We also describe the previously incomplete xiphiplastron, and analyze well-preserved trace marks on a plastral fragment.

Additional Uintan records of *Anosteira pulchra* from outside the study area are provided in *Table 2*. This set of specimens cannot be correlated with the measured stratigraphy of *Townsend, Friscia & Rasmussen (2006)*, but they demonstrate the presence of *A. pulchra* in other parts of the Uinta Basin, suggesting areas worthy of further collecting and stratigraphic analysis. UCMP locality V98069 is near Starvation Reservoir (Duchesne County, UT) and is partially surrounded by Uinta B and C strata (*Sprinkel, 2018*) (*Fig. 1*). Localities V71057 and V71058 are northwest of Ouray (Uintah County, UT), near Myton Pocket, and V98069 is near the study area, but not MWU localities (*Sprinkel, 2007*) (*Fig. 1*).



#### **Discussion & Conclusions**

#### Distribution of Anosteira pulchra in the Uinta Formation

Historically, most collecting in the Uinta Fm. has focused on mammals, and the most
frequently collected and most productive fossil mammal localities occur near the top and bottom
of the section (Townsend, Friscia & Rasmussen, 2006; Townsend et al., 2010) (Fig. 2A). It is
noteworthy that nearly all of the specimens collected and examined in this study were collected
from the surface or by traditional excavation techniques. Material from four locations at
approximately 280 m (Fig. 2A) was screenwashed but produced no turtle fossils. Since 2007,
more than 25 tons of bulk sample have been excavated from deposits at 237 m (Murphey et al.,
2017). This work has yielded more than 400 mammal specimens identifiable to genus or species
(Westgate et al., 2013). Only one Anosteira pulchra specimen (UMNH.VP.26554) was
recovered via these means, providing additional evidence that the taxon is uncommon or patchy
in distribution, rather than common and under sampled.
Based on the most common elements, the minimum number of the individuals (MNI) calculated
from the 95 <i>Anosteira pulchra</i> specimens reported in this study is 37. Of these, 78% occur above
140 m, in Uinta C sediments (Fig. 2A-B). The maximum abundance occurs near 237 m,
stratigraphically between the Glen Bench Bed and Sherbet Orange Bed (Fig. 2A-B). The most
significant gap is between the base of this interval (226 m) and the Uinta B-C boundary (137-140
m) (Fig. 2A). This interval contains the upper H section strata (below 200 m), which includes the
Ruby Red Wash, Red Wash Yellow, and Susan's Stripe Gray Marker Beds (Fig. 2A). The
remaining 22% of the MNI were found in Uinta B rocks, without a substantial peak as in higher
strata. Occurrences of A. pulchra in Uinta B are more evenly distributed and have lower
abundances than Uinta C. A gap in the uppermost Uinta B sediments near Devil's Playground 1



(106-137 m) is notable because this interval includes WU-117, a highly productive and well-sampled locality in the area. This suggests that the absence of *A. pulchra* fossils in the interval is not simply collection bias. Additional targeted collection in the future may reduce gaps, identify factors related to abundance, and clarify the trends reported here.

#### Evidence of rodent gnaw marks on UMNH.VP.26917

A hypoplastral fragment (UMNH.VP.26917) from 286 m (Uinta C) has four sets of linear excavations in the posterior half of its ventral surface, near the hypo-xiphiplastral suture (*Figs.* 4H, 5). The shell fragment is 24.4 mm long and 14.8 mm wide, consistent with the size of an adult turtle (*Fig.* 4H). Each of the foci has a thin puncture at its lateral end and several associated scrape marks which travel anteromedially across the bone to a maximum of 7.8 mm (*Fig.* 5). The scrape components are approximately perpendicular to the punctures and the ornamental ridges of the bone, nearly parallel and without intersection (*Fig.* 5). Scrapes are deepest near to the puncture and gradually become shallow medially, indicating that the wound was initiated laterally. The middle two punctures are most prominent, with shapes that are slightly sinusoidal and mirrored across the gap between them. The portions of the puncture nearest the gap are widest and deepest, penetrating the cortex. The anterior edges of each scrape are sharp and their floors rough, suggesting that the wounds had not undergone repair (*Fig.* 5).

The foci are interpreted as gnaw marks inflicted by a rodent, consistent with compression punctures and tapering scratches described on Eocene turtles by *Hutchison & Frye (2001)*. Rodent gnaw marks can be differentiated from those of carnivorans by their characteristic parallel series of furrows (*Haglund, Reay & Swindler, 1998; Pobiner, 2008*). The shape of the punctures indicates sharp flat teeth, consistent with rodent incisors, in addition to their small size (1.4-1.7 mm wide). The notable gap between the middle two foci (0.7 mm) suggests lower



390

368	incisors, which are sometimes not immediately adjacent due to the unfused mandibular
369	symphyses of rodents (Addison & Appleton, 1915; Weijs, 1975). No corresponding marks appear
370	on the dorsal side of the bone, suggesting the bites occurred before the turtle was macerated.
371	Rodents were common in a variety of sizes in Uinta C of the Uinta Fm. (see Rasmussen et al.,
372	1999), and the tracemaker was relatively small.
373	General remarks on shell structure and kinesis in Anosteira pulchra
374	The two North American species of Anosteira (A. ornata Leidy, 1871 and A. pulchra
375	Clark, 1932) are distinguished from one another primarily by the arrangement of neurals and
376	vertebral scales and the shape of the dorsal spines (Hay, 1906; Clark, 1932; Hutchison, 1996).
377	Both species of Anosteira (Clark, 1932) have a broadly ovate carapace with a shallow nuchal
378	embayment (Hay, 1908; Clark, 1932) (Fig. 3A-B). The plastral morphology of Anosteira is
379	similar to other trionychians, intermediate in size between the narrow, cruciform plastron of
380	Kizylkumemys and the large plastron of the Carettochelyinae (Havlik, Joyce & Böhme, 2014;
381	Joyce, 2014). The plastra of Anosteira spp. (and all Carettochelyidae) exhibit no visible sulci,
382	indicating that no plastral scales were present (Havlik, Joyce & Böhme, 2014; Joyce, 2014) (Figs.
383	4, 6B, D). Unlike Trionychidae, Anosteira features scales and sulci on the carapace, and has ten
384	pairs of peripherals (Havlik, Joyce & Böhme, 2014; Joyce, 2014) (Figs. 3, 6). The periphery of A.
385	pulchra forms a robust structural ring around the margin of the carapace (Fig. 6B, D). Sutures
386	between adjacent peripherals are generally articulated via fine dentate sutures, but many sutures
387	show broader and more diffuse areas of soft tissue connection, indicative of possible kinesis
388	(Bramble, 1974; Bramble, Hutchison & Legler, 1984; Angielczyk, Feldman & Miller, 2010). The

number of kinetic sutures and range of motion primarily enabled the head and neck to be

withdrawn under the carapace. Some flattening of the shell and the accommodation of relatively



394

395

396

397

398

399

400

401

402

403

404

405

406

407

408

409

410

411

412

413

enlarged fore flippers lateral to the shell were likely also permitted (*Bramble*, 1974; *Bramble*, 392 *Hutchison & Legler*, 1984).

#### Vertebral scale pattern variation in Anosteira pulchra

In general, carettochelyids exhibit a wide variety of scale patterns between genera, species and even individuals, and the clade is sexual dimorphic in body size and possibly posterior plastral kinesis (Joyce, Parham & Gauthier, 2004, 2012; Joyce, 2014; Danilov et al., 2017). The partial carapace of UMNH.VP.27146 (Figs. 3E, 7E) provides a clear example of the most common scale pattern recovered in the current study. Most published accounts of Anosteira pulchra (i.e., Clark, 1932; Gaffney, 1979; Havlik, Joyce & Böhme, 2014; Joyce, 2014; Danilov et al., 2017) are based on the holotype (CM 11808), which is a nearly complete carapace and plastron that is missing its entire anterior plastral lobe and most of the posterior lobe behind the hypo-xiphiplastral suture (Fig. 7A). CM 11808 has a pair of vertebral scales (the second and a coalesced third and fourth) that partly surround another between them, the anterior "additional vertebral" sensu Danilov et al., (2017). They are figured with a gap between them that occupies much of the length of costal 3 (see Figure 4 in *Danilov et al.*, 2017) (Fig. 7B). An examination of the type specimen (CM 11808) reveals that *Clark (1932)* accurately figured the pattern traced on the type specimen in red (Fig. 7A). However, except for UMNH.VP.31072, all fossil material discussed in the current study repeats a pattern in which there is contact between vertebral scale 2 and combined vertebral scales 3 and 4 (Figs. 3E, 7C-E). The degree of overlap is apparently somewhat variable, as evident when comparing the pattern of UMNH.VP.27146 (Fig. 7E) with two unpublished well-preserved carapaces (YPM VPPU 016317 and 016318) from the 1936 Princeton Uinta Basin expedition (Fig. 7C-D). The scute pattern of UMNH.VP.31072 is notable for lacking contact between vertebral 2 and vertebrals 3 + 4 (as in the type), and asymmetrical



constriction of the posterior extensions of vertebral 2 (*Fig. 7H*). However, contact between vertebrals 2 and 3 + 4 and sometimes slight overlap is the most frequently recovered variation (*Fig. 7C-E*). While this study presents a modified scale arrangement from the type, it is consistent with the homology and resulting discussion of carettochelyid phylogeny in *Danilov et al. (2017)*. It is unclear if the observed scale variation affected shell stability or is related to the broader carettochelyid trend of scale reduction and eventual loss. In any case, the longitudinal expansion of vertebral scales adjacent to the midline in *A. pulchra* is similar to that of *A. ornata (Danilov et al., 2017)*. However, *A. pulchra* still retains a unique morphology including additional vertebral scales to surround the costal-neural region, and new material clarifies the particular relationship between the only two known North American species. In total, this study provides a robust account of the morphology of *A. pulchra*, examines intraspecific variation of its vertebral scales, and expands its stratigraphic range into older Uintan strata. Future studies of stratigraphic distribution among the diverse turtle faunas of the Uinta Fm. may be useful in better understanding local and regional biostratigraphy during the Eocene.

#### **Acknowledgements**

Fossil collections from the Uinta Fm. were facilitated through permitting (permit to K.E.T.) and logistical assistance from the Bureau of Land Management. The authors would like to thank Dr. Rodney Scheetz of Brigham Young University Museum of Paleontology, Dr. Carrie Levitt-Bussian of the Natural History Museum of Utah, Dr. Steve Sroka of the Utah Field House of Natural History State Park Museum, Amy Henrici (Section of Vertebrate Paleontology) of the Carnegie Museum of Natural History, for their assistance in accessing and photographing specimens. Additional thanks to M. Kruback for photographic expertise on BYU specimens.



437	4	3	7
-----	---	---	---

Reference	S
-----------	---

430	References
439	Addison WHF, Appleton JL. 1915. The structure and growth of the incisor teeth of the albino rate
440	Journal of Morphology 26(1):43-96. https://doi.org/10.1002/jmor.1050260103
441	Angielczyk, KD, Feldman CR, Miller GR. 2010. Adaptive evolution of plastron shape in
442	emydine turtles. Evolution 65(2):377-394. https://doi.org/10.1111/j.1558-
443	5646.2010.01118.x
444	Batsch AJGC. 1788. Versuch einer Anleitung, zur Kenntniß und Geschichte der Thiere und
445	Mineralien, für akademische Vorlesungen entworfen, und mit den nöthigsten
446	Abbildungen versehen. Erster Theil. Allgemeine Geschichte der Natur; besondre der
447	Säugthiere, Vögel, Amphibien und Fische. Jena: Akademische Buchhandlung.
448	https://doi.org/10.5962/bhl.title.79854
449	Bramble DM. 1974. Emydid shell kinesis: biomechanics and evolution. <i>Copeia</i> 1974:707-727.
450	https://doi.org/10.2307/1442685
451	Bramble DM, Hutchison JH, Legler JM. 1984. Kinosternid shell kinesis: structure, function and
452	evolution. Copeia 1984(2):456-475. https://doi.org/10.2307/1445203
453	Broin F de. 1977. Contribution à l'étude des chéloniens: Chéloniens continentaux du Crétacé et
454	du Tertiaire de France. Paris: Éditions du muséum. Mémoires du Muséum National
455	d'histoire naturelle, nouvelle série, Series C, Sciences de la Terre 38:1-366.
456	Cashion WB. 1967. Geology and fuel resources of the Green River Formation, southeastern
457	Uinta Basin Utah and Colorado. U.S. Geological Survey Professional Paper 548:1-48.
458	https://doi.org/10.3133/pp548



159	Chamberlain CP, Mix, HT, Mulch A, Hren MT, Kent-Corson ML, Davis SJ, Horton TW,
160	Graham SA. 2012. The Cenozoic climate and topographic evolution of the western North
161	American Cordillera. American Journal of Science 312:213-262.
162	https://doi.org/10.2475/02.2012.5
163	Clark J. 1932. A new anosteirid from the Uinta Eocene. Annals of the Carnegie Museum 21:161-
164	170.
165	Cope ED. 1868. On some Cretaceous Reptilia. Proceedings of the Academy of Natural Sciences
166	of Philadelphia 1868:233-242.
167	Dane CH. 1954. Stratigraphic and facies relationships of the Upper part of Green River
168	Formation and Lower part of Uinta Formation in Duchesne, Uintah, and Wasatch
169	Counties, Utah. Bulletin of the American Association of Petroleum Geologists 38:405-
170	425. https://doi.org/10.1306/5ceadeea-16bb-11d7-8645000102c1865d
171	Dane CH. 1955. Stratigraphic and facies relationships of the upper part of the Green River
172	Formation and the lower part of the Uinta Formation in Duchesne, Uintah, and Wasatch
173	Counties, Utah. U.S. Geological Survey Chart OC-52. https://doi.org/10.3133/oc52
174	Danilov IC, Obraztsova EM, Chen W, Jin J. 2017. The cranial morphology of Anosteira
175	maomingensis (Testudines, Pancarettochelys) and the evolution of Pan-Carettochelyid
176	turtles. Journal of Vertebrate Paleontology 37(4):e1335735.
177	https://doi.org/10.1080/02724634.2017.1335735
178	Gaffney ES. 1979. Comparative cranial morphology of recent and fossil turtles. Bulletin of the
179	American Museum of Natural History 164(2):1-276.



480	Gill T. 1889. A remarkable tortoise. In: Annual Report of the Board of Regents of the
481	Smithsonian Institution, for the Year Ending June 30th, 1887, Pt. 1. Washington DC:
482	Government Printing Office, 509-511.
483	Gilmore CW. 1916. The fossil turtles of the Uinta Formation. Memoirs of the Carnegie Museum
484	7(2):1-82. https://doi.org/10.5962/bhl.title.44036
485	Gunnell GF, Murphey PC, Stucky RK, Townsend BKE., Robinson P, Zonneveld J-P, Bartels
486	WS. 2009. Biostratigraphy and biochronology of the latest Wasatchian, Bridgerian, and
487	Uintan North American Land Mammal "Ages". Museum of Northern Arizona Bulletin
488	65:279-330.
489	Havlik PE, Joyce WG, Böhme M. 2014. <i>Allaeochelys libyca</i> , a new carettochelyine turtle from
490	the middle Miocene of Libya. Bulletin of the Peabody Museum of Natural History
491	55:201-214. https://doi.org/10.3374/014.055.0207
492	Hay OP. 1906. On two interesting genera of Eocene turtles, Chisternon Leidy and Anosteira
493	Leidy. American Museum of Natural History Bulletin 22:155-160.
494	Hay OP. 1908. The Fossil Turtles of North America. Carnegie Inst. Washington Publications
495	75:1-568. https://doi.org/10.5962/bhl.title.12500
496	Haglund WD, Reay BS, Swindler DR. 1988. Tooth mark artifacts and survival of bones in
497	animal scavenged human skeletons. Journal of Forensic Sciences 33(4):985-997.
498	https://doi.org/10.1520/jfs12521j
499	Hummel K. 1929. Die fossilen Weichschildkroten (Trionychia). Eine morphologische-
500	systematische und stammesgeschichtliche. Studie. Geol. Palaeontol. 16:359-487.



01	Hutchison JH. 1996. Testudines. In: Prothero DR, Emery RJ, eds. <i>The Terrestrial Eocene</i> -			
502	Oligocene Transition in North America. Cambridge: Cambridge University Press, 337-			
503	353. https://doi.org/10.1017/CBO9780511665431			
504	Hutchison JH. 1998. Turtles across the Paleocene/Eocene Epoch Boundary in West-Central			
505	North America, p. 401-408. In: Aubry M-P, Lucas SG, Berggren WA, eds. Late			
506	Paleocene-Early Eocene climatic and biotic events in the marine and terrestrial records.			
507	Princeton: Princeton University Press.			
808	Hutchison JH, Frye FL. 2001. Evidence of pathology in early Cenozoic turtles. <i>PaleoBios</i>			
509	21(3):12-19.			
510	Joyce WG. 2014. A review of the fossil record of turtles of the clade Pan-Carettochelys. Bulletin			
511	of the Peabody Museum of Natural History 55:3-33.			
512	https://doi.org/10.3374/014.055.0102			
513	Joyce WG, Parham JF, and Gauthier JA. 2004. Developing a protocol for the conversion of rank-			
514	based taxon names to phylogenetically define clade names, as exemplified by turtles.			
515	Journal of Paleontology 78(5):989-1013. https://doi.org/10.1666/0022-			
516	3360(2004)078<0989:dapftc>2.0.co;2			
517	Joyce WG, Micklich N, Schaal SFK, Scheyer TM. 2012. Caught in the act: the first record of			
518	copulating fossil vertebrates. Biology Letters 8:846-848.			
519	https://doi.org/10.1098/rsb1.2012.0361			
520	Joyce WG, Lyson TR. 2015. A review of the fossil record of turtles of the clade Baenidae.			
521	Bulletin of the Peabody Museum of Natural History 56(2):147-183.			
522	https://doi.org/10.3374/014.056.0203			



523	Joyce WG, Volpato VS, Rollot Y. 2018. The skull of the carettochelyid turtle Anosteira pluchra			
524	from the Eocene (Uintan) of Wyoming and the carotid canal system of carettochelyid			
525	turtles. Fossil Record 21:301-310. https://doi.org/10.5194/fr-21-301-2018			
526	Leidy J. 1871. [Remarks on some extinct turtles from Wyoming Territory]. Proceedings of the			
527	Academy of Natural Sciences of Philadelphia 1871:102-103.			
528	8 Murphey PC, Townsend KEB, Friscia AR, Evanoff E. 2011. Paleontology and stratigraphy of			
529	9 middle Eocene rock units in the Bridger and Uinta Basins, Wyoming and Utah. <i>The</i>			
530	Geological Society of America Field Guide 21:1-42.			
531	https://doi.org/10.1130/2011.0021(06)			
532	Murphey PC, Townsend KEB, Friscia AR, Westgate J, Evanoff E, Gunnell GF. 2017.			
533	Paleontology and stratigraphy of Middle Eocene Rock Units in the Southern Green River			
534	and Uinta Basins, Wyoming and Utah. Geology of the Intermountain West 4:1-53.			
535	https://doi.org/10.31711/giw.v4i0.11			
536	Osborn HF. 1895. Fossil mammals of the Uinta Basin—expedition of 1894. Bulletin of the			
537	American Museum of Natural History 7(2):71-105.			
538	Osborn HF. 1929. The Titanotheres of ancient Wyoming, Dakota, and Nebraska. U.S.			
539	Geological Survey Monograph 55(1):1-701. https://doi.org/10.3133/m55			
540	Prothero DR. 1996. Magnetic stratigraphy and biostratigraphy of the middle Eocene Uinta			
541	Formation, Uinta Basin, Utah. In: Prothero DR, Emry RJ, eds. The Terrestrial Eocene-			
542	Oligocene Transition in North America. Cambridge: Cambridge University Press, 3-24.			
543	https://doi.org/10.1017/cbo9780511665431.002			
544	Pobiner B. 2008. Paleoecological information in predator tooth marks. <i>Journal of Taphonomy</i>			
545	6(3-4):373-397.			



546	Rasband WS. 1997-2016. ImageJ. Bethesda: U. S. National Institutes of Health.			
547	Rasmussen DT, Conroy GC, Friscia AR, Townsend KE, Kinkel MD. 1999. Mammals of the			
548	middle Eocene Uinta Formation. In: Gillette DD, ed. Vertebrate Paleontology in Utah:			
549	Utah Geological Survey Miscellaneous Publication 99-1. Salt Lake City: Utah Geological			
550	Survey, 401-420.			
551	1 Ray RG, Kent BH, Dane CH. 1956. Stratigraphy and photogeology of the southwestern part of			
552	the Uinta Basin, Duchesne and Uintah Counties, Utah. U.S. Geological Survey Oil and			
553	Gas Investigations Map OM-171.			
554	Riggs ES. 1912. New or little known titanotheres from the lower Uintah formations—with notes			
555	on the stratigraphy and distribution of fossils. Field Museum of Natural History			
556	Publication 159(2):17-41. https://doi.org/10.5962/bhl.title.3381			
557	Ryder RT, Fouch TD, Elison JH. 1976. Early Tertiary sedimentation in the western Uinta Basin,			
558	Utah. GSA Bulletin 87:469-512. https://doi.org/10.1130/0016-			
559	7606(1976)87<496:etsitw>2.0.co;2			
560	Smith HF, Hutchison JH, Townsend KEB, Adrian B, Jager D. 2017. Morphological variation,			
561	phylogenetic relationships, and geographic distribution of the Baenidae (Testudines),			
562	based on new specimens from the Uinta Formation (Uinta Basin), Utah (USA). PLoS			
563	ONE. https://doi.org/10.1371/journal.pone.0180574: 1-40.			
564	Smith HF, Jager D, Hutchison JH, Adrian B, Townsend KEB. 2020. Epiplastral and geographic			
565	variation in Echmatemys, a geoemydid turtle from the Eocene of North America: A			
566	multi-tiered analysis of epiplastral shape complexity. Paleobios			
567	37.ucmp_paleobios_46852: 1-14.			



568	Sprinkel DA. 2007. Interim geologic map of the Vernal 30' x 60' Quadrangle, Uintah and			
569	Duchesne Counties, Utah and Moffat and Rio Blanco Counties, Colorado. Utah			
570	Geological Survey Open-File Report 506DM: Plate 1.			
571	Sprinkel DA. 2018. Interim geologic map of the Duchesne 30' x 60' Quadrangle, Duchesne and			
572	Wasatch Counties, Utah. Utah Geological Survey Open-File Report OFR-689: Plate 1.			
573	73 Stidham TA, Townsend KEB, Holroyd PA. 2020. Evidence for wide dispersal in a stem			
574	galliform clade from a new small-sized middle Eocene pangalliform (Aves:			
575	Paraortygidae) from the Uinta Basin of Utah (USA). Diversity 12(90):1-13.			
576	6 https://doi.org/10.3390/d12030090			
577	7 Townsend KEB, Friscia AR, Rasmussen DT. 2006. Stratigraphic distribution of upper middle			
578	Eocene fossil vertebrate localities in the Eastern Uinta Basin, Utah, with comments on			
579	Uintan biostratigraphy. The Mountain Geologist 43(2):115-134.			
580	Townsend KEB, Rasmussen DT, Murphey PC, Evanoff E. 2010. Middle Eocene habitat shifts in			
581	the North American western interior: A case study. Palaeogeography,			
582	Palaeoclimatology, Palaeoecology 297:144-158.			
583	https://doi.org/10.1016/j.palaeo.2010.07.024			
584	Weijs WA. 1975. Mandibular movements of the albino rat during feeding. <i>Journal of</i>			
585	Morphology 145(1):107-124. https://doi.org/10.1002/jmor.1051450107			
586	Westgate J, Townsend KEB, Cope D, Gartner C. 2013. Progress report on the first Uinta C			
587	micro-mammal fauna from the Uinta Basin and its comparison with the Casa Blanca			
588	mammal community from Laredo, Texas. Geological Society of America Abstracts with			
589	Programs. Denver: Geological Society of America:325.			



590	Wood HE, Chaney RW, Clark J, Colbert EH, Jepsen GL, Reeside JB, Stock C. 1941.
591	Nomenclature and correlation of the North American continental Tertiary. Geological
592	Society of America Bulletin 52:1-48. https://doi.org/10.1130/gsab-52-1
593	
594	Additional Information
595	Funding
596	Funding for this research was provided by Midwestern University faculty intramural funds (to
597	K.E.T).
598	Competing Interests
599	The authors declare there are no competing interests.
600	Author Contributions
501	• Brent Adrian analyzed the data, wrote the paper, prepared figures and/or tables, reviewed
602	drafts of the paper.
603	• Patricia A. Holroyd reviewed drafts of the paper and prepared Figure 1.
604	• J. Howard Hutchison reviewed drafts of the paper.
605	• K.E. Beth Townsend reviewed drafts of the paper and prepared Table 1.
606	
607	Captions
808	Figure 1. Index map of Utah and collection sites of <i>Anosteira pulchra</i> in the current study.
609	Figure 2. Stratigraphic distribution of A. pulchra in the upper Uinta Fm. (A) Stratigraphic
610	sections indicating marker unit correlation of the six sections of the Uinta Fm. (Townsend,
611	Friscia & Rasmussen, 2006). (B) Minimum number of A. pulchra individuals. Green rectangle
312	corresponds with meter level range for WU-34 (226-248 m). (C) Correlation of the measured



613	stratigraphic section of Townsend, Friscia & Rasmussen (2006) relative to the Global Magnetic
614	Polarity Time scale, using magnetostratigraphic section of <i>Townsend et al. (2010)</i> and <i>Prothero</i>
615	(1996).
616	Figure 3. Carapace material of <i>Anosteira pulchra</i> from the Uinta Fm. (A-B) Dorsal (left) and
617	ventral (right) views of UMNH.VP.27632, an articulated nuchal and left first peripheral. (C)
618	Right lateral view of UMNH.VP.31059, an articulated neural 3 and 4. (D) Left lateral view of
619	UMNH.VP.27146, a partial articulated carapace. (E-F) Dorsal (left) and ventral (right) views of
620	a partial carapace, UMNH.VP.27146. (G-I) Dorsal (left), ventral (center), and lateral (right)
621	views of UMNH.VP.30590, neurals 6 and 7. (J-L) Dorsal (left), ventral (center), and lateral
622	(right) views of pygal and suprapygal from the same specimen. (M-N) Dorsal (left) and ventral
623	(right) views of UMNH.VP.19951, a right costal 1. (O-Q) Dorsal (left), ventral (center), and
624	posterior (right) views of UMNH.VP.31058, a right peripheral 2. (R-T) Dorsal (left), ventral
625	(center), and anterior (right) views of UMNH.VP.27077, a left peripheral 3. (U-X) Dorsal (left),
626	ventral (left center), medial (right center), and posterior (right) views of UMNH.VP.27077, a left
627	peripheral 6. (Y-AA) Dorsal (left), ventral (center), and anterior (right) of UMNH.VP.30590, a
628	right peripheral 8. Dotted black lines indicate edges of missing bone, vertical blue lines indicate
629	orientation of the midline, and purple lines indicate sulci. UMNH.VP specimen numbers are in
630	rectangles. All parts of figure to same scale. Abbreviations: ne= neural, nu= nuchal, py= pygal,
631	sp= suprapygal.
632	Figure 4. Plastral material of Anosteira pulchra from the Uinta Fm. (A-B) Ventral (left), and
633	dorsal (right) views of UMNH.VP.19551, a partial left plastron. (C-D) Ventral (left) and dorsal
634	(right) views of a UMNH.VP.27452, a nearly complete left hypoplastron. (E-G) Ventral (left),
635	medial (center), and dorsal (right) views of UMNH.VP.26554, a partial left hypoplastron. (H-I)



636	Ventral (left), and dorsal (right) views of UMNH.VP.26917, a partial right hypoplastron with			
637	probably rodent gnaw marks circled in red. (J-M) Ventral (left), dorsal (left center), medial (right			
638	center), and lateral (right) views of UMNH.VP.20525, a nearly complete right xiphiplastron.			
639	UMNH.VP specimen numbers are in rectangles. All parts of figure to same scale. Dotted black			
640	lines indicate edges of missing bone and vertical blue lines indicate orientation of the midline.			
641	Figure 5. Magnified ventral surface of hypoplastral fragment UMNH.VP.26917, showing traces			
642	of rodent incisors (indicated by arrows) near the hypo-xiphiplastron suture. Scale shows 1 mm			
643	increments and black arrows indicate orientation.			
644	Figure 6. Associated carapace and plastron of <i>Anosteira pulchra</i> , specimen UMNH.VP.31072.			
645	(A) Vertebral series and suprapygal in dorsal view. (B) Plastron and peripheral ring in dorsal			
646	view. (C) Vertebral series and suprapygal in ventral view. (D) Plastron and peripheral ring in			
647	ventral view. All parts of figure to same scale. Vertical blue lines indicate orientation of the			
648	midline. Abbreviations: ne= neural, nu= nuchal, py= pygal, sp= suprapygal.			
649	<b>Figure 7.</b> Scale pattern variation within <i>Anosteira pulchra</i> . (A) Dorsal carapace of CM 11808,			
650	type specimen of A. pulchra. (B) Detail of carapacial scale pattern of CM 11808 as previously			
651	published (Clark, 1932), with red lines indicating sulci, black lines indicating sutures, and yellow			
652	star indicating unmarked region of shell. (C) Detail of carapacial scale pattern of YPM VPPU			
653	16318. (D) Detail of carapacial scale pattern of YPM VPPU 16317. (E) Partial carapace with			
654	scale pattern of UMNH.VP.27146. (F) Scale pattern of neural spike of larger individual in			
655	dorsolateral view of UMNH.VP.27453. (G) Scale pattern of third neural of smaller individual in			
656	dorsolateral view of UMNH.VP.27453. (H) Scale pattern of partial carapace of			
657	UMNH.VP.31072 in dorsal view. Scale bar applies to CM 11808 only.			





658	<b>Table 1.</b> Uinta Fm. Anosteira pulchra specimens by stratigraphic meter level. * indicates a BYU
659	locality that is not assigned a meter level.
660	<b>Table 2.</b> Anosteira pulchra records from the Uinta Fm. outside of the measured stratigraphic
661	section of Townsend, Friscia & Rasmussen (2006)



#### Table 1(on next page)

Uinta Fm. Anosteira specimens by stratigraphic meter level.

Uinta Fm. *Anosteira* specimens by stratigraphic meter level. \* indicates a BYU locality that is not assigned a meter level.



- 1 **Table 1.** Uinta Fm. *Anosteira* specimens by stratigraphic meter level. \* indicates a BYU locality
- 2 that is not assigned a meter level.

Specimen	MWU	Meter	
	locality	Level	Element
UMNH.VP.27635	WU-123	366	Shell fragments
UMNH.VP.27634	WU-49	364	Neurals; many shell fragments
UMNH.VP.27212	WU-49	364	Shell fragments
UMNH.VP.27077	WU-50	361	Left peripherals 3, 6
	WU-50		Left peripheral 7; right hypoplastron fragment;
UMNH.VP.27202		361	articulated right nuchal/peripheral 1
UMNH.VP.27146	WU-50		Partial left hypoplastron; right peripherals 1-2,
		361	possible 4, 10; neurals 2-4, 6; costals 3-5
UFH 2002.19.2	WU-185	334	Partial carapace including neural
UFH 2002.19.3	WU-185	334	Shell fragments
UMNH.VP.27299	WU-223	332	Pygal
UMNH.VP.27307	WU-223		Right peripheral 6, 8, 10; pygal; possible left
			hyoplastron frag; partial right xiphiplastron; 1
		332	possible right hypoplastral fragment
UMNH.VP.26539	WU-223	332	Left peripherals 5-6
UMNH.VP.26917	Above		
	WU-216	286	Right hypoplastron fragment
UMNH.VP.26919	Above		
	WU-216	286	Superpygal



ID OHI VD 26504	A 1		
UMNH.VP.26504	Above		
	WU-216	286	Partial pygal; partial peripheral
UMNH.VP.26920	Above		
	WU-216	286	Plastron fragment
UMNH.VP.26511	Above		
	WU-216	286	Carapace fragments
UMNH.VP.18945	WU-45	285	Plastron and carapace fragments
UMNH.VP.20505	WU-216		Right peripherals 1, 6-7; partial neural; costal
		284	fragments
UMNH.VP.20506	WU-216	284	Partial hypoplastron
UMNH.VP.20518	WU-216	284	Carapace fragments
UMNH.VP.20498	WU-216	284	Pygal; costal fragments; posterior hypoplastron
UMNH.VP.20479	WU-216	284	Carapace fragments
UMNH.VP.20496	WU-216	284	Partial nuchal; partial costal; partial hyoplastron
UMNH.VP.20525	WU-216		Partial costals; left peripherals 1-6, right
		284	peripherals 4-6; pygal; right xiphiplastron
UMNH.VP.20523	WU-216	284	Right peripheral 6
UMNH.VP.20522	WU-216	284	Right peripheral 6
UMNH.VP.20532	WU-216	284	Carapace fragments
UMNH.VP.20533	WU-216	284	Carapace and plastron fragments
UMNH.VP.20535	WU-216	284	Carapace and plastron fragments
UMNH.VP.20536	WU-216	284	Carapace and plastron fragments
UMNH.VP.20537	WU-216	284	Carapace and plastron fragments



UMNH.VP.20538	WU-216	284	Carapace and plastron fragments
UMNH.VP.20539	WU-216	284	Carapace and plastron fragments
UMNH.VP.20540	WU-216	284	Carapace and plastron fragments
UMNH.VP.20541	WU-216	284	Carapace and plastron fragments
UMNH.VP.20542	WU-216	284	Carapace and plastron fragments
UMNH.VP.20543	WU-216	284	Carapace and plastron fragments
UMNH.VP.20551	WU-216	284	Carapace and plastron fragments
UMNH.VP.20552	WU-216	284	Carapace and plastron fragments
UMNH.VP.20553	WU-216	284	Carapace and plastron fragments
UMNH.VP.17724	WU-121	282	Carapace fragments
UMNH.VP.30592	WU-34	226-248	Partial peripherals; small fragments
UMNH.VP.30593	WU-34	226-248	Small fragments
UMNH.VP.30594	WU-34	226-248	Partial peripherals; many small fragments
UMNH.VP.30595	WU-34	226-248	Left peripherals 5, 6, 8; plastron fragment
UMNH.VP.27424	WU-34	226-248	Pygal; partial peripherals; shell fragments
UMNH.VP.20582	WU-34	226-248	Carapace fragments
UMNH.VP.20583	WU-34	226-248	Carapace fragments
UMNH.VP.20584	WU-34	226-248	Carapace fragments
UMNH.VP.30596	WU-34	226-248	Costal fragments; peripherals
UMNH.VP.30597	WU-34	226-248	Neurals 2-3; plastron fragments
UMNH.VP.30598	WU-34		Pygal; peripheral fragments; carapace fragments;
		226-248	plastron fragments
UMNH.VP.30599	WU-34	226-248	Neural; partial peripheral; fragments
			1



UMNH.VP.30600	WU-34		Neural 5 or 6; right peripherals 5-6; left
			peripherals 3-6; left possible hyoplastron
			fragment; anterior peripherals; carapace
		226-248	fragments; plastron fragments
UMNH.VP.30602	WU-34		Left peripheral 5; left possible hypoplastron
		226-248	fragment; indet. plastron fragment.
UMNH.VP.30603	WU-34	226-248	Costals; neurals
UMNH.VP.30604	WU-34		Articulated partial anterior carapace including
		226-248	nuchal
UMNH.VP.30605	WU-34		Neurals 2-4; anterior peripheral; partial
		226-248	peripheral; many tiny fragments
UMNH.VP.27450	WU-34	226-248	Peripheral; shell fragments
UMNH.VP.27452	WU-34	226-248	Pygal; left hypoplastron
UMNH.VP.30586	WU-34	226-248	Many small fragments
UMNH.VP.30587	WU-34	226-248	Many costal fragments
UMNH.VP.30588	WU-34	226-248	Partial left hypoplastron
UMNH.VP.30589	WU-34	226-248	Partial peripherals; small fragments
UMNH.VP.30590	WU-34	226-248	Right peripheral 8, neurals 6-7, pygal, suprapygal
UMNH.VP.30591	WU-34	226-248	Left and right peripheral 1
UMNH.VP.30910	WU-34	226-248	Neurals 2-3
UMNH.VP.27226	WU-34	226-248	Small fragments (mostly plastron)
UMNH.VP.27453	WU-34		Partial pygal; partial nuchal; partial peripherals;
		226-248	small fragments



UMNH.VP.27630	WU-34	226-248	Plastral fragments	
UMNH.VP.27454	WU-34	226-248	Right xiphiplastron fragment	
UMNH.VP.27632	WU-34	226-248	Nuchal; left peripheral 1	
UMNH.VP.26515	WU-26	237	Many small plastron fragments	
UMNH.VP.26554	WU-26		Neurals 1-3; partial left hypoplastron; probable	
		237	femora; partial peripherals; many tiny fragments	
UMNH.VP.31070	WU-26	237	Partial peripherals; many fragments	
UMNH.VP.31058	WU-26	237	Peripheral 2; partial costals; small fragments	
UMNH.VP.31059	WU-26	237	Neurals 3-4; small fragments	
UMNH.VP.31060	WU-26	237	Partial peripherals; small fragments	
UMNH.VP.26556	WU-26	237	Bridge peripherals	
UMNH.VP.19951	WU-12	141	Right costal 1	
UMNH.VP.27281	WU-1		3 possible individuals; Partial peripherals; shell	
		106	fragments; 3 pygals; right peripheral 1	
UMNH.VP.20034		*	Shell fragments	
UMNH.VP.20405		*	Partial hypoplastron, partial costal	
UMNH.VP.20231		*	Plastron and carapace fragments	
UMNH.VP.30607	WU-54	96	Peripheral 2	
UMNH.VP.30606	WU-54	96	Posterior peripherals	
UMNH.VP.30601	WU-54		Bilateral hyoplastra, indeterminate partial costal,	
		96	40 carapace fragments	
UMNH.VP.18943	WU-32	>95	Plastron and carapace fragments	
UMNH.VP.18935	WU-32	>95	Plastron and carapace fragments	
		t.		



UMNH.VP.20661	WU-32	>95	Right peripherals 6, 7
UMNH.VP.27306	WU-23		Left and right peripheral 5; posterior peripheral
		~83	fragments
UMNH.VP.31072	WU-8	57-60	Associated partial carapace and plastron
UMNH.VP.31073	WU-8	57-60	Pygal
UMNH.VP.27243	WU-18		2 individuals; partial peripherals; plastron
			fragments; pygals; left hypoplastron;
		25	indeterminate shell fragments



#### Table 2(on next page)

Anosteira pulchra records from the Uinta Fm. outside of the measured stratigraphic section of Townsend, Friscia & Rasmussen (2006).

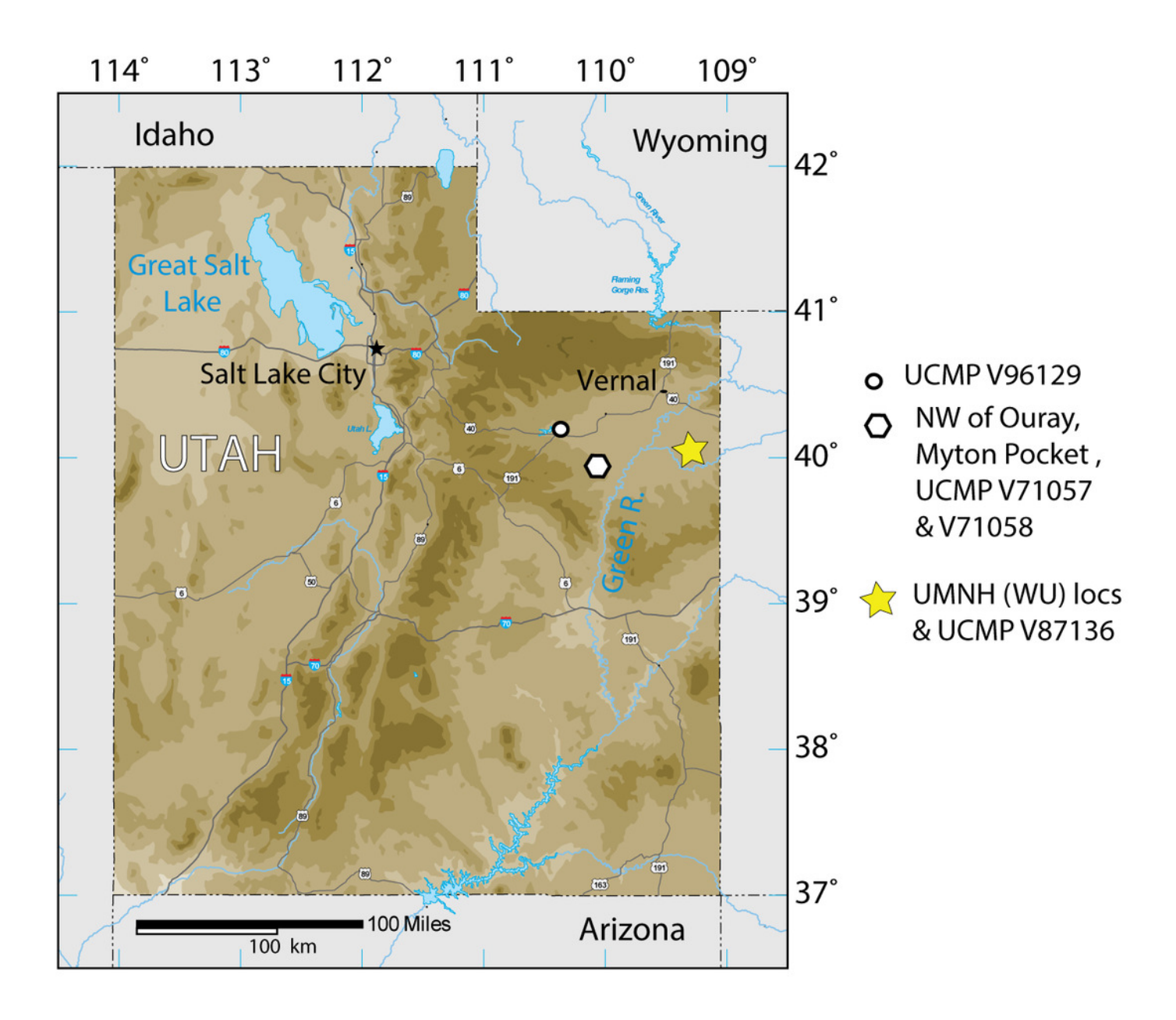
Anosteira pulchra records from the Uinta Fm. outside of the measured stratigraphic section of Townsend, Friscia & Rasmussen (2006).



- 1 Table 2. Anosteira pulchra records from the Uinta Fm. outside of the measured stratigraphic
- 2 section of Townsend, Friscia & Rasmussen (2006).

Specimen	Locality	Element
UCMP 218731	V98069	Shell fragments
UCMP 223356	V98069	Hyo- or hypoplastral
		fragment
UCMP 223357	V98069	Hyo- or hypoplastral
		fragment
UCMP 223358	V98069	Bridge peripheral
UCMP 223359	V98069	Peripheral
UCMP 223360	V98069	Peripheral
UCMP 223361	V98069	Peripheral
UCMP 235587	V98069	Bridge peripheral
UCMP 235588	V87136	Left hyoplastron and
		shell fragments
UCMP 223098	V71057	Peripheral 2
UCMP 223099	V71057	Peripheral 8
UCMP 218732	V71058	Shell fragments
UCMP 223355	V71058	Shell fragments

Index map of Utah and collection sites of *Anosteira pulchra* in the current study.

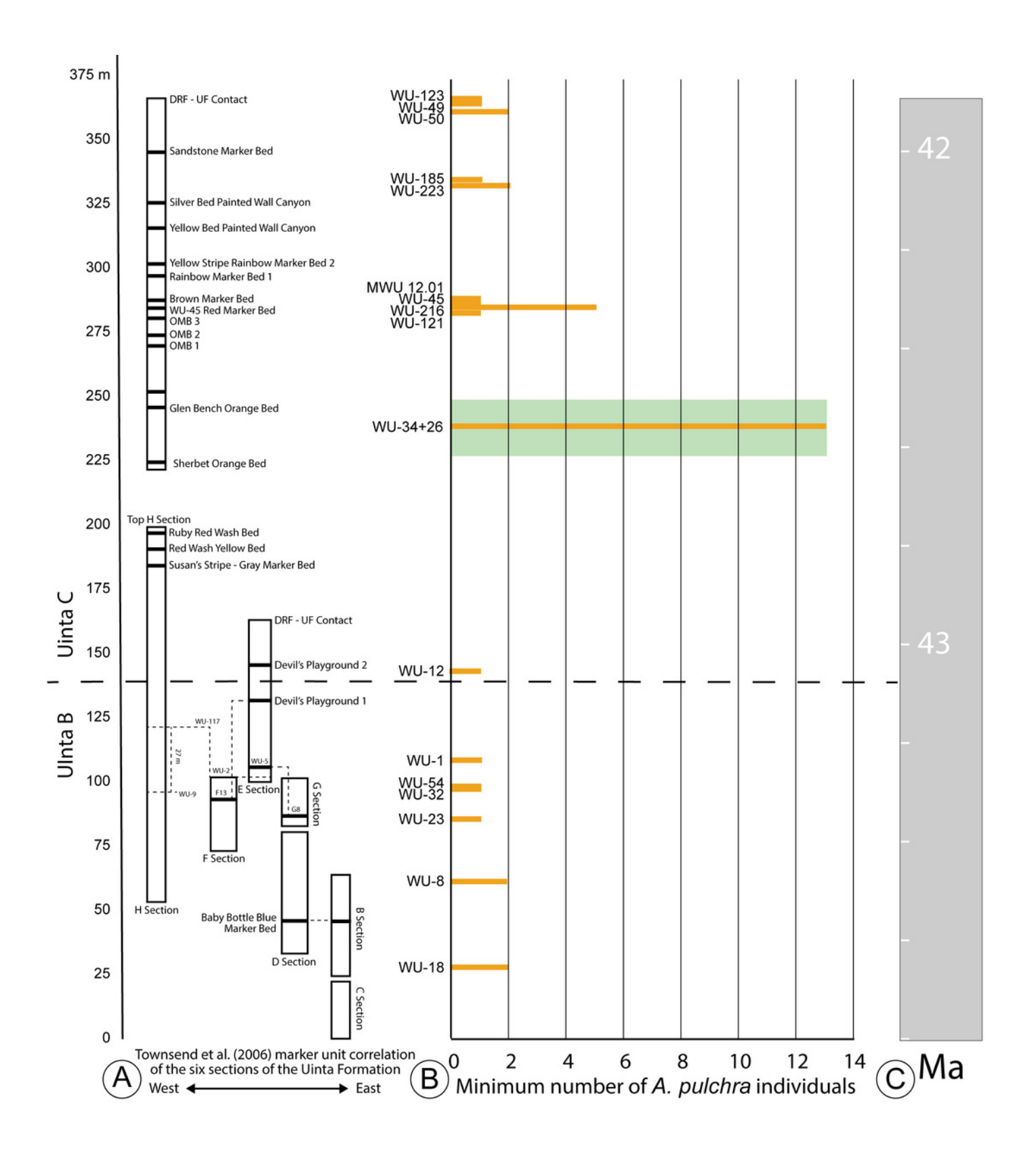




Stratigraphic distribution of A. pulchra in the upper Uinta Fm.

(A) Stratigraphic sections indicating marker unit correlation of the six sections of the Uinta Fm. (*Townsend, Friscia & Rasmussen, 2006*). (B) Minimum number of *A. pulchra* individuals. Green rectangle corresponds with meter level range for WU-34 (226-248 m). (C) Correlation of the measured stratigraphic section of *Townsend, Friscia & Rasmussen* (2006) relative to the Global Magnetic Polarity Time scale, using magnetostratigraphic section of *Townsend et al.* (2010) and *Prothero* (1996).



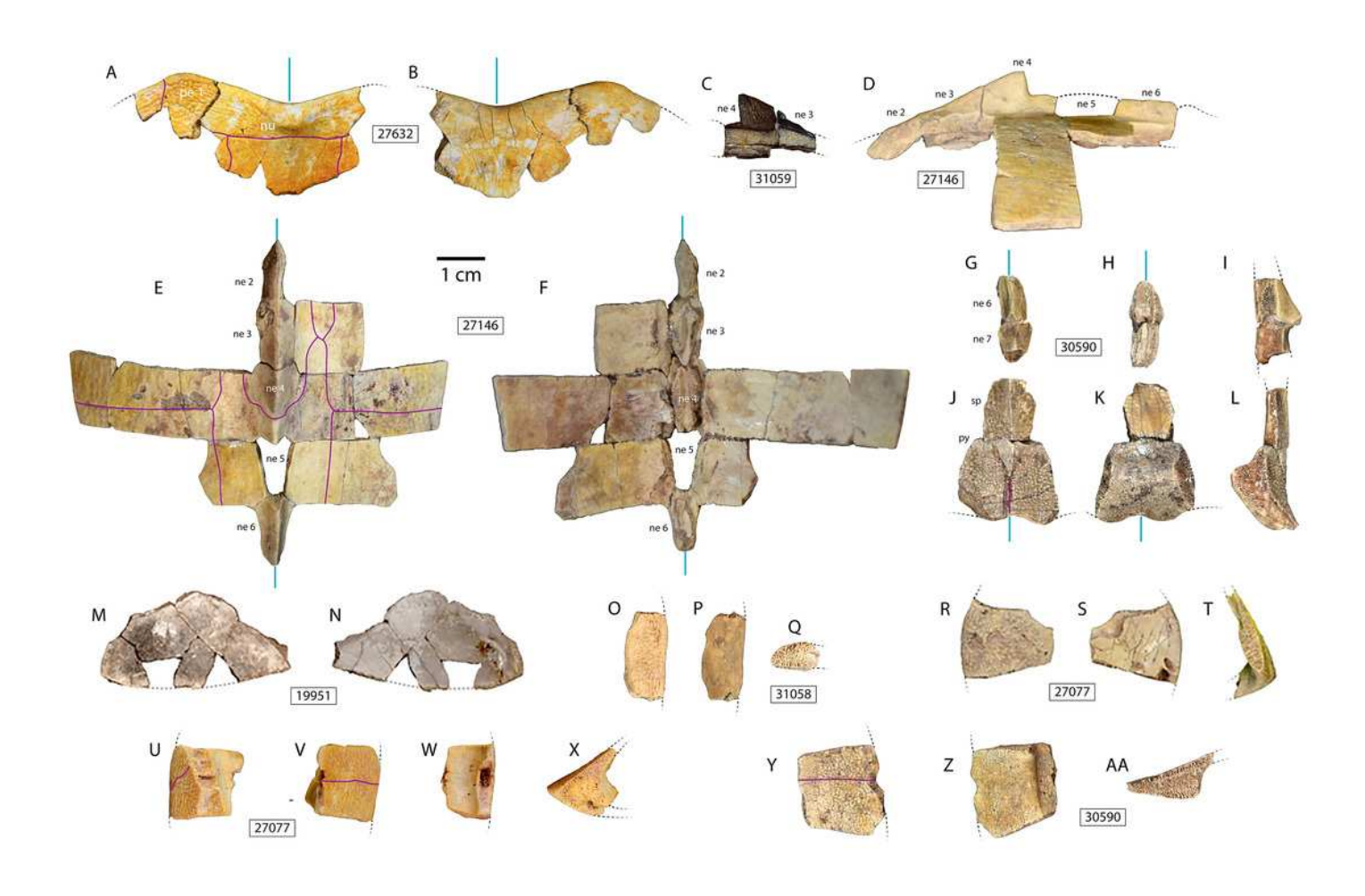




Carapace material of *Anosteira pulchra* from the Uinta Fm.

(A-B) Dorsal (left) and ventral (right) views of UMNH.VP.27632, an articulated nuchal and left first peripheral. (C) Right lateral view of UMNH.VP.31059, an articulated neural 3 and 4. (D) Left lateral view of UMNH.VP.27146, a partial articulated carapace. (E-F) Dorsal (left) and ventral (right) views of a partial carapace, UMNH.VP.27146. (G-I) Dorsal (left), ventral (center), and lateral (right) views of UMNH.VP.30590, neurals 6 and 7. (J-L) Dorsal (left), ventral (center), and lateral (right) views of pygal and suprapygal from the same specimen. (M-N) Dorsal (left) and ventral (right) views of UMNH.VP.19951, a right costal 1. (O-Q) Dorsal (left), ventral (center), and posterior (right) views of UMNH.VP.31058, a right peripheral 2. (R-T) Dorsal (left), ventral (center), and anterior (right) views of UMNH.VP.27077, a left peripheral 3. (U-X) Dorsal (left), ventral (left center), medial (right center), and posterior (right) views of UMNH.VP.27077, a left peripheral 6. (Y-AA) Dorsal (left), ventral (center), and anterior (right) of UMNH.VP.30590, a right peripheral 8. Dotted black lines indicate edges of missing bone, vertical blue lines indicate orientation of the midline, and purple lines indicate sulci. UMNH.VP specimen numbers are in rectangles. All parts of figure to same scale. Abbreviations: ne= neural, nu= nuchal, py= pygal, sp= suprapygal.

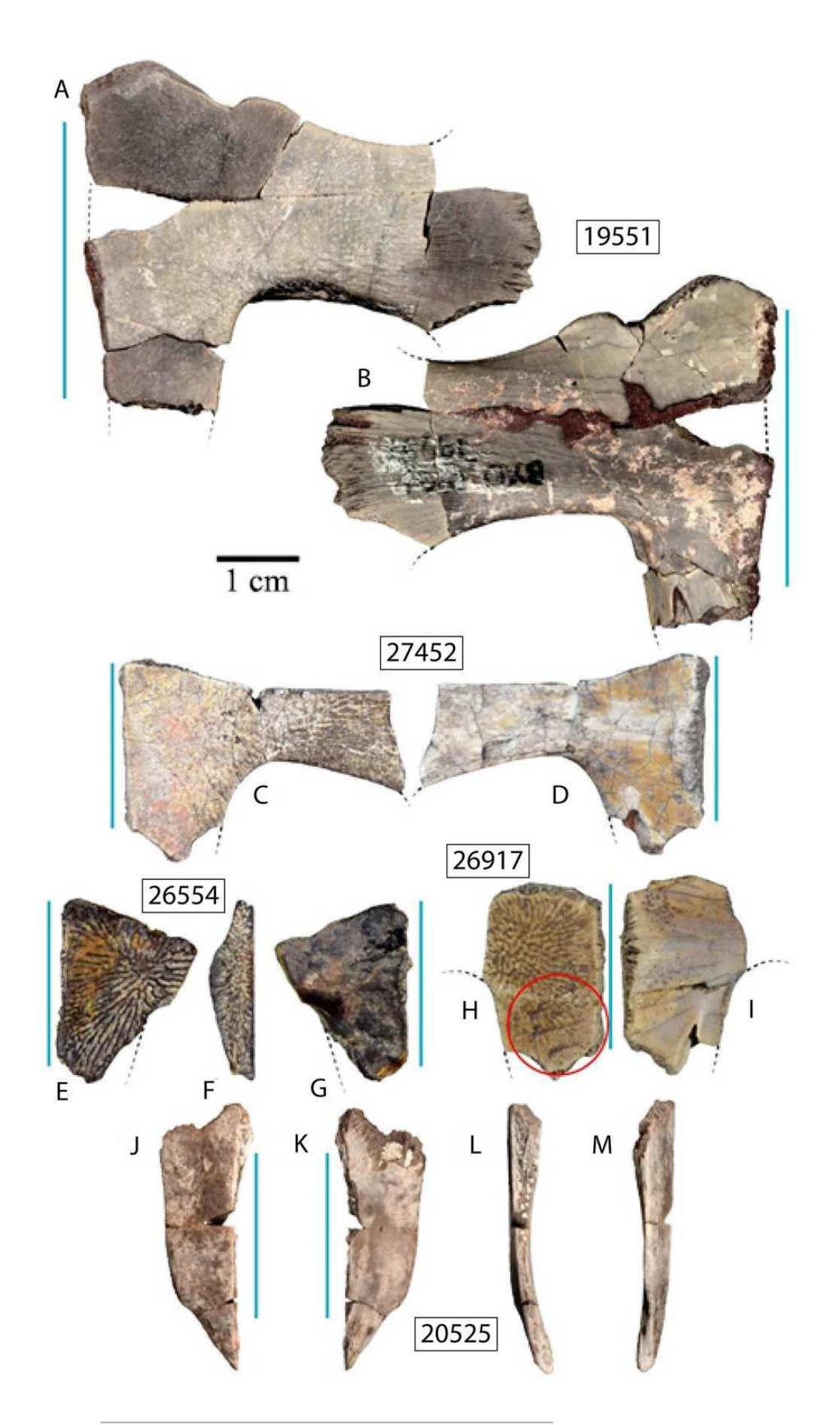






Plastral material of Anosteira pulchra from the Uinta Fm.

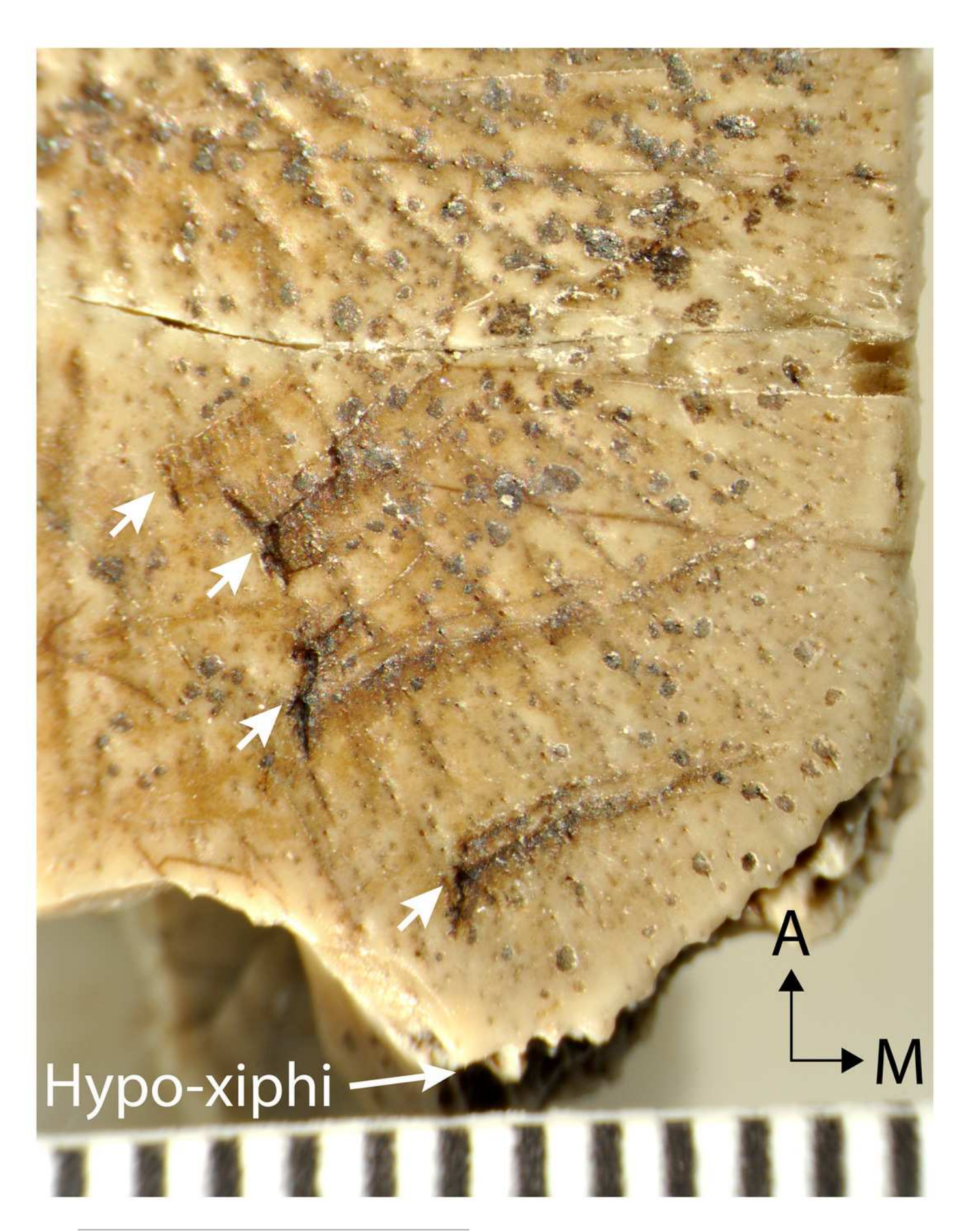
(A-B) Ventral (left), and dorsal (right) views of UMNH.VP.19551, a partial left plastron. (C-D) Ventral (left) and dorsal (right) views of a UMNH.VP.27452, a nearly complete left hypoplastron. (E-G) Ventral (left), medial (center), and dorsal (right) views of UMNH.VP.26554, a partial left hypoplastron. (H-I) Ventral (left), and dorsal (right) views of UMNH.VP.26917, a partial right hypoplastron with probably rodent gnaw marks circled in red. (J-M) Ventral (left), dorsal (left center), medial (right center), and lateral (right) views of UMNH.VP.20525, a nearly complete right xiphiplastron. UMNH.VP specimen numbers are in rectangles. All parts of figure to same scale. Dotted black lines indicate edges of missing bone and vertical blue lines indicate orientation of the midline.





Magnified ventral surface of hypoplastral fragment UMNH.VP.26917, showing traces of rodent incisors (indicated by arrows) near the hypo-xiphiplastron suture.

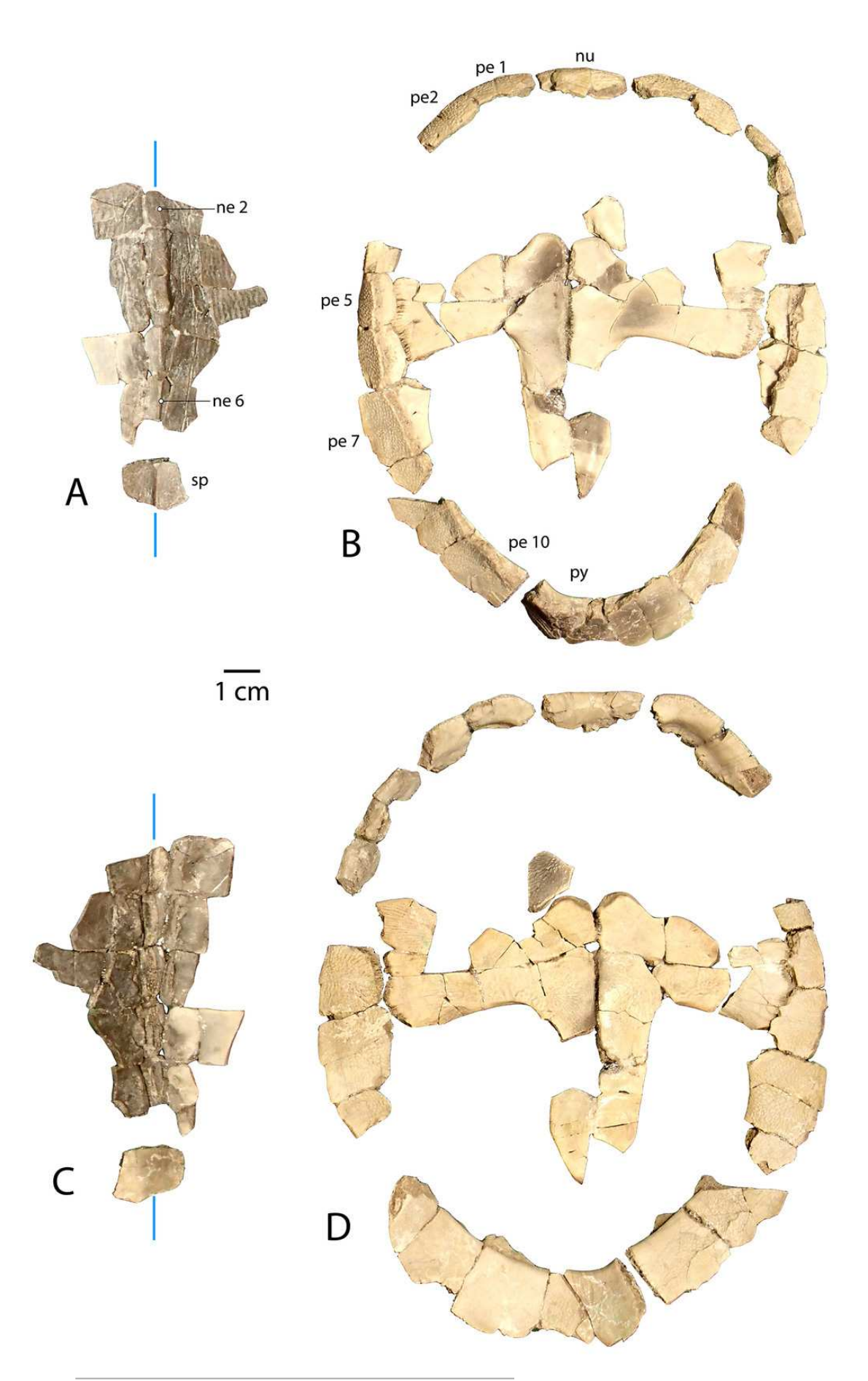
Scale shows 1 mm increments and black arrows indicate orientation.





Associated carapace and plastron of Anosteira pulchra, specimen UMNH.VP.31072.

(A) Vertebral series and suprapygal in dorsal view. (B) Plastron and peripheral ring in dorsal view. (C) Vertebral series and suprapygal in ventral view. (D) Plastron and peripheral ring in ventral view. All parts of figure to same scale. Vertical blue lines indicate orientation of the midline. Abbreviations: ne= neural, nu= nuchal, py= pygal, sp= suprapygal.



Scale pattern variation within Anosteira pulchra.

(A) Dorsal carapace of CM 11808, type specimen of *A. pulchra*. (B) Detail of carapacial scale pattern of CM 11808 as previously published (*Clark, 1932*), with red lines indicating sulci, black lines indicating sutures, and yellow star indicating unmarked region of shell. (C) Detail of carapacial scale pattern of YPM VPPU 16318. (D) Detail of carapacial scale pattern of YPM VPPU 16317. (E) Partial carapace with scale pattern of UMNH.VP.27146. (F) Scale pattern of neural spike of larger individual in dorsolateral view of UMNH.VP.27453. (G) Scale pattern of third neural of smaller individual in dorsolateral view of UMNH.VP.27453. (H) Scale pattern of partial carapace of UMNH.VP.31072 in dorsal view. Scale bar applies to CM 11808 only.

